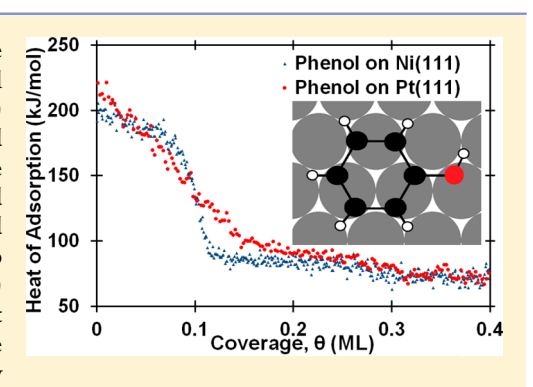
Article

pubs.acs.org/JPCC

# Energetics of Adsorbed Phenol on Ni(111) and Pt(111) by Calorimetry

- 3 Spencer J. Carey, Wei Zhao, De Zhongtian Mao, and Charles T. Campbell De Campbell To Campbell De Cam
- 4 University of Washington, Box 351700, Seattle, Washington 98195-1700, United States

**ABSTRACT:** The heat of adsorption and sticking probability of phenol were measured on Ni(111) at 150 K and Pt(111) at 90 K using single crystal adsorption calorimetry (SCAC). Phenol adsorbs molecularly on both Ni(111) and Pt(111), with an initial heat adsorption of 200. kJ/mol on Ni(111) and 220 kJ/mol on Pt(111). The integral heat of adsorption at 1/9 ML coverage (–176 kJ/mol for Ni(111) and –175 kJ/mol for Pt(111)) gives a standard enthalpy of formation ( $\Delta H_{\rm f}^0$ ) for C<sub>6</sub>H<sub>5</sub>OH<sub>ad</sub> of –272 kJ/mol on Ni(111) and –271 kJ/mol on Pt(111). The measured bonding energies for phenol to Ni(111) and Pt(111) were compared to density functional theory (DFT) calculations from previous literature, showing that DFT functionals that included van der Waals corrections are more accurate, although some calculations on both surfaces, even those with vdW corrections, still grossly underestimated the adsorption energy.



#### INTRODUCTION

5

6

10

11

12

13

14

15

16

19 Phenol is the simplest example of an aromatic oxygenate, a class 20 of compounds that are involved in many important catalytic 21 and electrocatalytic reactions on late transition metal surfaces. 22 As such, it is often studied as a model compound to understand 23 surface reactions for this class of compounds. For example, 24 phenol is often used as a model for studying catalytic and 25 electrocatalytic biomass conversion reactions over Pt, Ni, and 26 other late transition metals. <sup>1–5</sup> In order to better understand 27 how phenol behaves in catalytic reactions, it is critical to know 28 the energetics of phenol on catalyst surfaces. Here, we report 29 the first calorimetric measurements of the adsorption energy of 30 phenol on any transition metal surface, and extract from these 31 the bond energies and heats of formation of phenol adsorbed 32 on two model catalyst surfaces, Ni(111) and Pt(111).

Phenol adsorption onto Ni(111) has been studied with temperature-programmed desorption (TPD), vibrational spec-35 troscopy (RAIRS), and Auger electron spectroscopy (AES). These methods found that phenol chemisorbs molecularly parallel to the surface, interacting through its  $\pi$ -bonds with the surface. Multilayers of phenol already start desorbing at the lowest adsorption temperature studied (170 K). The first layer mainly decomposes during TPD, as evidenced by desorption peaks for H<sub>2</sub> (starting at ~300 K) and CO (starting at ~420 K).

Phenol adsorption on Pt(111) has been studied with vibrational spectroscopy (HRELS), <sup>7–9</sup> low-energy electron diffraction (LEED), AES, TPD, <sup>7,9</sup> and X-ray photoelectron spectroscopy (XPS). Below 200 K, phenol adsorbs molecu-47 larly, parallel to the surface. <sup>7–9</sup> At low temperatures, multilayers are formed that possess a desorption peak at 195 K. There is a transition (second) layer between the chemisorbed first layer and multilayers that interacts weakly with the Pt(111) surface. The adsorption energy of this layer is slightly stronger than the

multilayer, as evidenced by a TPD desorption peak at 225 K. $^9$  52 At 200 K, adsorbed phenol dissociates by O–H bond scission, 53 resulting in phenoxy and an adsorbed hydrogen atom.  $^{7,9}$  54 Further analysis shows that phenoxy transitions to a  $\eta^5$ - $\pi$ - 55 adsorption or oxocyclohexadienyl species.  $^9$  By 490 K, this 56 species decomposes to CO and H $_2$  gas, plus some carbon 57 residue on the surface.  $^9$ 

## **■ EXPERIMENTAL SECTION**

Experiments were performed in a UHV chamber (base pressure 60 <2  $\times$  10<sup>-10</sup> mbar) equipped with XPS, AES, low-energy ion 61 scattering spectroscopy (LEIS), LEED, and SCAC. The sample 62 used was a 1  $\mu$ m thick Ni(111) or Pt(111) single-crystal foil, 63 supplied by Jacques Chevallier at Aarhus University in 64 Denmark. The sample surface was cleaned by Ar<sup>+</sup> ion 65 sputtering and annealing to remove contaminants. This 66 treatment was repeated until impurities were below the 67 detection limit of XPS, and the surface gave a very sharp 68 LEED pattern. Detailed descriptions of the apparatus, 69 molecular beam, sticking probability, heat measurements, and 70 other procedures for SCAC may be found elsewhere.  $^{10-13}$ 

Briefly, calorimetry was performed by holding the clean 72 metal single crystal at a given temperature and exposing it to a 73 pulsed molecular beam of phenol. The heat of adsorption was 74 measured with a pyroelectric detector pressed against the 75 backside of the sample. The sensitivity of the pyroelectric 76 detector was calibrated after each experiment by depositing a 77 known amount of energy into the sample by use of a HeNe 78

Special Issue: Hans-Joachim Freund and Joachim Sauer Festschrift

Received: April 3, 2018 Revised: May 10, 2018 Published: May 10, 2018



79 (632.8 nm) laser. The sticking probability was measured 80 simultaneously with the heat of adsorption using a quadrupole 81 mass spectrometer, as described previously. 15 We report two 82 types of sticking probabilities, long term and short term. 12 The 83 long-term sticking probability,  $S_{\infty}$ , is the probability that a gas 84 molecule strikes the Ni(111) or Pt(111) surface, sticks, and 85 remains until the next gas pulse starts ~3 s later. This 86 measurement is used to calculate the adsorbate coverage 87 remaining at the start of the next gas pulse. The short-term 88 sticking probability,  $S_{102\text{ms}}$ , is the probability that a gas molecule 89 strikes the Ni(111) or Pt(111) surface, sticks, and remains at 90 least throughout the time frame of our heat measurement (i.e., 91 the first 102 ms). This is used to calculate the moles of gas-92 phase reactant that contribute to the measured heat of 93 adsorption, so we can report that value in kilojoules per mole 94 adsorbed.

The molecular beam was created by expanding  $\sim$ 0.3 mbar of 96 phenol (Sigma-Aldrich, >99%) through a microchannel array 97 held at 300  $\pm$  5 K (defining the gas temperature) and then 98 collimated through a series of five liquid-nitrogen-cooled 99 orifices. A chopper converts the beam into pulses that are 100 102 ms long and repeat every 3 s. Coverages are reported in 101 monolayers (ML) and are defined as the number of phenol 102 molecules that adsorb to the surface irreversibly, normalized by 103 the number of metal surface atoms in the Ni(111) surface (1.86  $\times$  10<sup>15</sup> Ni atoms/cm<sup>2</sup>) or Pt(111) surface (1.50  $\times$  10<sup>15</sup> Pt 105 atoms/cm<sup>2</sup>). A typical phenol dose was  $\sim$ 0.001–0.002 ML per 106 pulse with a beam spot size previously determined to be 4.36 107 mm in diameter. <sup>10</sup>

#### 108 RESULTS

Sticking Probability. As described previously  $^{12}$  and above, we measured two types of sticking probabilities: the short-term sticking probability,  $S_{102\text{ms}}$ , and the long-term sticking probability,  $S_{\infty}$ . Figure 1 shows the average short-term and

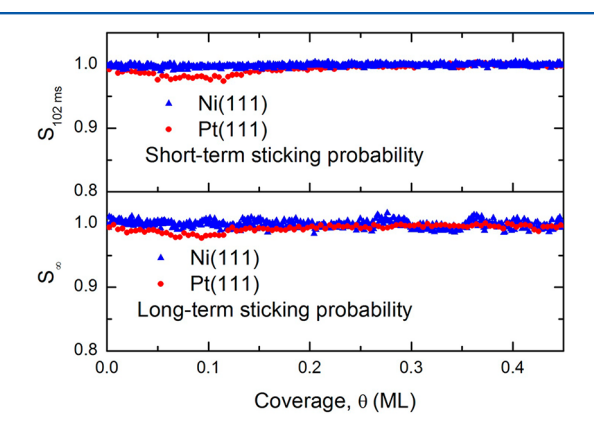


Figure 1. Average short-term and long-term sticking probabilities of phenol versus coverage at 90 K for Pt(111) and 150 K for Ni(111).

113 long-term sticking probabilities measured as a function of 114 coverage on both Ni(111) and Pt(111). At these low 115 temperatures, the sticking probability is near unity for both 116 metal surfaces independent of coverage. On both surfaces, 117 multilayer formation is expected and confirmed in this work.  $^{6,9}$  118 For Ni(111), both sticking probabilities start and remain very 119 near unity for all experiments. For Pt(111), the initial short-120 term and long-term sticking probabilities start near unity but 121 decrease slightly over the first 0.1 ML of coverage to  $\sim$ 0.98 and 122 then increase to near unity at coverages above 0.15 ML after

the first layer saturates (see below). The lower sticking 123 probability in the first layer on Pt(111) than in the multilayer 124 or on Ni(111) may be due to poorer mass-matching in the gas- 125 surface collision on Pt(111), as proposed for a similar 126 observation for benzene on Pt(111). Poorer mass-matching 127 in the gas—surface collisions results in a higher probability for 128 quasi-elastic collisions and hence lower trapping probability. 17 129

Heat of Adsorption of Molecular Phenol on Ni(111) at  $^{130}$  150 K. In this paper, we define the term heat of adsorption as  $^{131}$  the negative of the differential standard molar enthalpy change  $^{132}$  for the adsorption reaction,  $\Delta H_{\rm ad}$ , with the gas and the metal  $^{133}$  surface being at the same temperature as the metal surface  $^{134}$  ("standard" here implies only that the gas is at 1 bar as a pure  $^{135}$  ideal gas). During our experiments, the temperature of the  $^{136}$  molecular beam was  $^{\sim}300$  K, while the Ni(111) sample was  $^{137}$  held at cryogenic temperatures (e.g., T=150 K). Thus, the  $^{138}$  measured heat is corrected by the small difference in the  $^{139}$  internal energy of the gas in the directed molecular beam at its  $^{140}$  source temperature ( $^{300}$  K) and in a Boltzmann distribution at  $^{141}$  the sample temperature ( $^{T}$ ) and then by RT to convert from  $^{142}$  internal energy change to enthalpy change for the adsorption  $^{143}$  reaction, as described elsewhere.

Figure 2 shows the heat of adsorption of phenol on the  $^{145}$   $^{12}$  Ni(111) surface at 150 K. Under these conditions, phenol is  $^{146}$ 

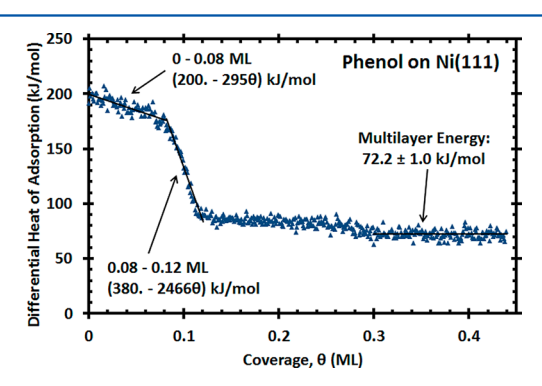


**Figure 2.** Differential heat of adsorption of molecularly adsorbing phenol on Ni(111) at 150 K as a function of adsorbed phenol coverage. Each data point represents a pulse of  $\sim$ 0.001 ML of phenol gas.

expected to adsorb molecularly, parallel to the surface.<sup>6</sup> Phenol 147 initially adsorbs with a heat of 200 kJ/mol. As the coverage 148 increases to 0.08 ML, the heat of adsorption decreases linearly 149 with coverage and is well described by the best-fit line  $-\Delta H_{ad} = 150$  $(200.-295 \theta)$  kJ/mol, where  $\theta$  is the coverage in ML. At 0.08 151 ML, the negative slope abruptly increases in magnitude. From 152 0.08 to 0.115 ML, the heat of adsorption is well described by 153 the linear best-fit line  $-\Delta H_{ad} = (380-2466 \,\theta)$  kJ/mol. At 0.115 154 ML, the negative slope abruptly decreases in magnitude to near 155 zero. Between 0.115 and ~0.28 ML, the heats of adsorption 156 remain almost constant at approximately 85 kJ/mol. This 157 indicates that there exists a transition layer between bulk 158 multilayer phenol and the first chemisorbed layer. By 0.30 ML, 159 we form multilayers of bulk phenol and the heat of adsorption 160 becomes constant at  $72.2 \pm 1.0$  kJ/mol, where the error bars 161 are the run-to-run standard deviation on the mean of the 162 average heat from 0.30 to 0.45 ML. This agrees well with the 163 literature values for the heat of sublimation of phenol. 164 Averaging the three literature values given by NIST gives a 165 standard heat of sublimation of 69.0 kJ/mol at 298 K. 19-21 166 Using the gas phase and solid phase heat capacities of phenol, 167

168 this average may be adjusted to the experiment temperature of 169 150 K, giving a standard enthalpy of sublimation of 71.2 kJ/170 mol. This value agrees within 1 kJ/mol of our measured value. 171 These measurements indicate that the first layer of 172 chemisorbed phenol is completed at 0.115 ML, which is within 173 the error of the ideal coverage of 1/9 ML for a  $(3 \times 3)$  174 structure. Thus, each phenol occupies approximately nine Ni 175 atoms at saturation. To the best of our knowledge, there is no 176 information as to whether phenol forms an ordered structure 177 on the Ni(111) surface. The saturation coverage of benzene on 178 Ni(111) is 0.13 ML (i.e., 7.7 Ni atoms per benzene) at 90 K. 16 This larger area per phenol is not surprising, since it has the 180 extra OH group.

Heat of Adsorption of Molecular Phenol on Pt(111) at 90 K. Figure 3 shows the heat of adsorption of phenol on the

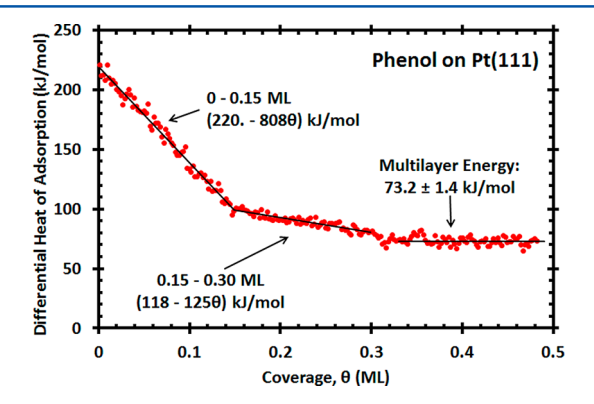


Figure 3. Differential heat of adsorption of molecularly adsorbing phenol on Pt(111) at 90 K as a function of adsorbed phenol coverage. Each data point represents a pulse of  $\sim$ 0.002 ML of phenol gas.

183 Pt(111) surface at 90 K. Here, phenol is expected to initially 184 adsorb molecularly, parallel to the surface. The Phenol adsorbs 185 initially with a heat of adsorption of 220 kJ/mol. From 0–0.15 186 ML, the heat of adsorption decreases linearly with coverage and 187 is well described by the best-fit line  $-\Delta H_{\rm ad} = (220-808~\theta)~{\rm kJ/188}~{\rm mol.}$  Our saturation coverage of the first layer is within error of 189 that expected for a  $(\sqrt{7}\times\sqrt{7})~{\rm R19.1}^{\circ}$  structure, which 190 corresponds to a coverage of  $1/7=0.143~{\rm ML.}$  Lu et al. 191 adsorbed phenol from aqueous solutions onto a Pt(111) 192 electrode at room temperature and observed a  $(3\times3)$  193 structure at saturation using LEED and HREELS, which 194 corresponds to 1/9 ML. Our coverage in UHV may be larger 195 due to the absence of water solvent and the lower adsorption 196 temperature used here.

From 0.15-0.30 ML, the heat of adsorption decreases much 197 198 more slowly and is well described by the best-fit line  $-\Delta H_{\rm ad}$  = (118–125  $\theta$ ) kJ/mol. The presence of this transition layer 200 agrees well with previous TPD experiments, which found that the second phenol layer binds slightly more strongly, compared to bulk multilayer phenol, by evidence of a higher desorption peak at 225 K (compared to 195 K for the multilayer). By 0.3 ML, bulk-like multilayers of phenol are formed and the 205 heat of adsorption becomes constant at  $73.2 \pm 1.4 \text{ kJ/mol}$ where the error bars are the run-to-run standard deviation on 207 the mean of the average heat from 0.30 to 0.48 ML. Adjusting 208 the standard enthalpy of sublimation reported for bulk phenol 209 (solid) at 298  $\rm K^{19-21}$  to 90 K using the gas phase and solid 210 phase heat capacities of phenol results in a literature enthalpy of 211 71.9 kJ/mol. This value agrees within 1.3 kJ/mol with the heat 212 of multilayer adsorption measured in this work.

#### DISCUSSION

**Energetics of Adsorbed Phenol.** The measured enthalpy 214 of molecular adsorption at 150 K on Ni(111) (Figure 2) and at 215 90 K on Pt(111) (Figure 3) may be used to calculate the heats 216 of formation of phenol on both surfaces. These heats for 217 Ni(111) and Pt(111) are compared directly in Figure 4, and 218 f4

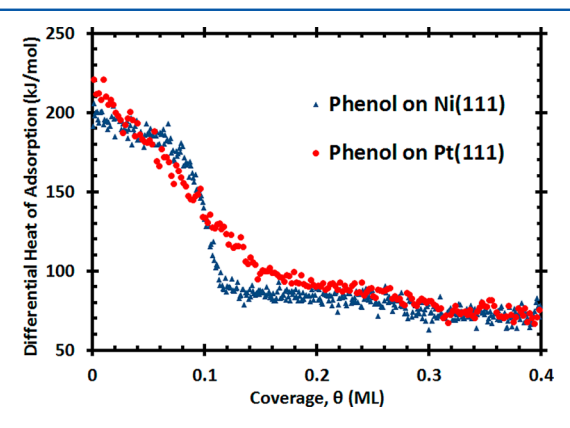
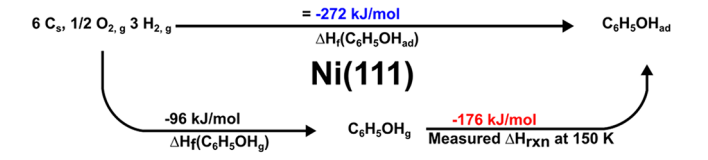


Figure 4. Comparison of the differential heat of adsorption of phenol on Ni(111) at 150 K and Pt(111) at 90 K as a function of adsorbed phenol coverage.

seen to be similar. We use the integral heat determined from 219 the best fit lines for each adsorption curve up to a coverage of 220 1/9 ML. The thermodynamic cycles in Figure 5 show how to 221 fs



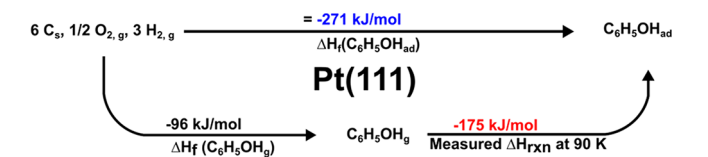


Figure 5. Reactions used to determine the heat of formation of molecularly adsorbed phenol on the Ni(111) and Pt(111) surfaces. The values in red correspond to the integral enthalpy of adsorption measured at 90 K for Ni(111) and 150 K for Pt(111) for the first 1/9 ML of coverage. The values in blue correspond to the resulting heats of formation of adsorbed phenol ( $C_6H_5OH_{ad}$ ).

extract the heats of formation of adsorbed phenol on both 222 Ni(111) and Pt(111). On the left-hand side of the figure, all 223 elements are in their standard states and therefore possess a 224 heat of formation of zero. The first step at the bottom is simply 225 the enthalpy of formation of gaseous phenol,  $-96~\rm kJ/mol.^{19-21}$  226 The second step at the bottom is our integral enthalpy of 227 adsorption measured by SCAC from 0 to 1/9 ML of coverage 228 ( $-176~\rm kJ/mol$  for Ni(111) and  $-175~\rm kJ/mol$  for Pt(111)). 229 Adding these values together results in the enthalpy of 230 formation of adsorbed phenol, i.e., the top pathway:  $-272~\rm 231~\rm kJ/mol$  for Ni(111) and  $-271~\rm kJ/mol$  for Pt(111).

Since there is no decomposition of phenol in these 233 experiments, our measured integral heat of adsorption is 234 equal to the total phenol—metal bond enthalpy. Therefore, at 235

Table 1. Comparison of Present Calorimetric Integral Bond Energies of Phenol to Ni(111) at 150 K and Pt(111) at 90 K with Calculated Values at 0 K Using DFT with Periodic Boundary Conditions

phenol on Ni(111)			bond energy (kJ/mol)		reference
coverage	DFT functional/method	DFT site	DFT	calorimetry	DFT
1/9 ML	PBE	bridge	88	175	25
1/16 ML	PBE-D3 (includes vdW)	HCP hollow	96	190	26
phenol on Pt(111)			bond energy (kJ/mol)		reference
coverage	DFT functional/method	DFT site	DFT	calorimetry	DFT
1/25 ML	PW91	bridge	215	203	27
1/16 ML	PBE	bridge	112	194	28
1/16 ML	PBE	bridge	126	194	29
1/16 ML	PBE-vdW	HCP hollow	176	194	29
1/16 ML	revPBE-vdW	HCP hollow	105	194	29
1/16 ML	PW86-vdW2	HCP hollow	100	194	29
1/16 ML	PBE-dDsC	bridge	208	194	30
1/16 ML	optB88-vdW	bridge	199	194	28
1/16 ML	PBE-D3 (includes vdW)	HCP hollow	172	194	26

236 1/9 ML coverage, the phenol—Ni(111) bond enthalpy is —176 237 kJ/mol and the phenol—Pt(111) bond enthalpy is —175 kJ/238 mol. These bond enthalpies may be converted into bond 239 energies by changing sign and subtracting RT. This results in a 240 phenol—Ni(111) bond energy of 175 kJ/mol and phenol—241 Pt(111) bond energy of 174 kJ/mol, both averaged up to 1/9 242 ML.

Previous TPD work studying adsorbed phenol on Pt(111) 244 shows a clearly resolved peak at 225 K, which corresponds to a 245 second layer, above the 195 K peak for multilayer phenol. This 246 second layer, with a slightly higher heat of adsorption than the 247 multilayer, is also clearly observed in Figure 3. Averaging the 248 data points in Figure 3 from 0.15 to 0.30 ML gives an average 249 adsorption enthalpy of 89.5 kJ/mol for this second layer. 250 Converting this value to an activation energy of desorption 251 ( $E_{\rm des}$ ) by subtracting  $^{1}/_{2}$ RT (as explained elsewhere  $^{22}$ ) gives 252  $E_{\rm des}$  = 89.1 kJ/mol. Using this  $E_{\rm des}$  in the first-order Redhead 253 equation 22 together with its reported TPD peak temperature of 254 225 K gives a prefactor for desorption of this second layer of 255  $2.5 \times 10^{20}$  s $^{-1}$ .

Comparison of Phenol Adsorption on Ni(111) and 257 Pt(111). A direct comparison of the heats of adsorption of 258 phenol on Ni(111) at 150 K and Pt(111) at 90 K is shown in 259 Figure 4. On the basis of the bond energies measured in this 260 work, phenol binds with comparable bond strength to both 261 surfaces. The 1 kJ/mol difference in the integral bond energy at 262 1/9 ML is well within the error in our absolute calibration (up to 3%). 11 By "integral bond energy" here, we mean the average adsorption energy between zero coverage and the stated coverage, or 1/9 ML here. However, this difference changes 266 depending on the chosen coverage. Initially, phenol binds to 267 Pt(111) more strongly than Ni(111), up to a coverage of ~0.04 ML. From ~0.04 to ~0.10 ML, the differential heat of adsorption of phenol on Ni(111) is stronger. The higher heat below 0.04 ML on Pt may be due to a larger fraction of step sites on Pt(111), the removal of which requires higher annealing temperatures than Ni(111). Step sites are known to bind aromatic molecules more strongly than terraces on Pt(111).<sup>23</sup> From ~0.10 ML up until the saturation of the second layer, phenol binds stronger to Pt(111) again.

The similarity in first-layer heats of phenol adsorption between Ni(111) and Pt(111) above was also seen for benzene. This was explained for benzene as being due to a

cancellation of two opposing effects: stronger intrinsic covalent 279 bonding for Ni–C compared to Pt–C bonds but stronger van 280 der Waals (vdW) attractions for Pt. The similarity for phenol 281 is not surprising, since the nature of the bonding seems to be 282 very similar to that of benzene, as indicated by the similar 283 integral bond energies for benzene  $(166.9 \text{ kJ/mol at } 1/9 \text{ ML on } 284 \text{ Ni}(111) \text{ and } 160.7 \text{ kJ/mol at } 1/9 \text{ ML on Pt}(111))^{16} \text{ compared } 285 \text{ to those above for phenol. There seems to be little contribution } 286 \text{ to the adsorption energy from oxygen-to-metal bonds, since } 287 \text{ O-Ni bonds should be } 50 \text{ kJ/mol stronger than } \text{O-Pt } 288 \text{ bonds.}^{24}$ 

adsorption of phenol onto Ni(111) and Pt(111) measured in 291 this work may be used as benchmarks for comparison to 292 theoretical calculations. Table 1 gives several calculated bond 293 the energies from various DFT methods and the measured integral 294 bond energy of adsorbed phenol at the same coverage. As 295 reviewed in the Introduction, previous experimental measure-296 ments on both Ni(111) and Pt(111) had indicated that the 297 phenol adsorbs molecularly (without bond breaking) with its 298 aromatic ring lying parallel to the metal surface under the 299 conditions of the present calorimetric measurements. The DFT 300 results here are also for such a structure. They do not include 301 zero-point energy corrections. The DFT results for each surface are divided into two sections, those that employ corrections for 303 van der Waals (vdW) forces and those that do not.

The calculated DFT results for phenol adsorption on 305 Ni(111) underestimate the adsorption energy strength by 306 87-94 kJ/mol, regardless of the inclusion of vdW corrections, 307 which was done with only one functional, PBE-D3. The 308 calculated DFT results for phenol adsorption on Pt(111) range 309 from underestimating the energy by 94 kJ/mol to over- 310 estimating the energy by 12 kJ/mol. Results that include vdW 311 corrections were less likely to underestimate the energy. 312 However, in some cases, vdW-corrected functionals also 313 underestimated the adsorption energy to Pt(111) by ~100 314 kJ/mol. For the closely related system of benzene on Ni(111), 315 optB86b-vdW and optB88-vdW gave adsorption energies of 316 211 and 173 kJ/mol, respectively, both close to our SCAC 317 value of 188 kJ/mol. 16 Therefore, we believe that the very low 318 value for the DFT energy on Ni(111) for the one study that 319 included vdW corrections in Table 1 is probably due to a 320 problem with that particular method (PBE-D3) for Ni(111), 321

388

322 rather than due to a general problem with vdW corrections in 323 DFT for Ni(111). As seen in Table 1, this same method only 324 underestimates the adsorption energy for Pt(111) by 22 kJ/325 mol

The experiments in Table 1 are at 150 and 90 K, whereas the 327 DFT values are for 0 K. The heat capacity difference between 328 solid phenol and gaseous phenol is only 14 J/(mol K) at 150 K 329 and drops to  $\sim 10 \text{ J/(mol K)}$  at 90 K,  $^{31}$  and this difference must 330 approach zero at 0 K. Thus, we expect the average heat capacity 331 difference between adsorbed phenol and gaseous phenol to be 332 <30 J/(mol K) in the range from 0 K to the measurement 333 temperature of 90 or 150 K. Thus, the temperature difference 334 between the experiments and the DFT results in Table 1 335 should contribute less than 5 kJ/mol to the energy differences 336 seen there.

To the best of our knowledge, there is no experimental knowledge of the preferred adsorption site of phenol on either superface. Theoretical studies that do not include vdW corrections systematically calculate the strongest adsorption to be at bridge sites. Studies that use vdW corrected functionals vary in their adsorption site, preferring either bridge or HCP hollow sites. For phenol, the adsorption site is defined as the site over which the aromatic ring is centered.

# 45 CONCLUSIONS

346 On Ni(111), phenol adsorbs molecularly at 150 K with a 347 decreasing heat of adsorption in the first 0.08 ML well fit by 348  $-\Delta H_{\rm ad} = (200-295~\theta)~{\rm kJ/mol}$ . From 0.08 to 0.115 ML, the 349 heat of adsorption drops more rapidly and is well fit by  $-\Delta H_{\rm ad}$  350 =  $(386-2529~\theta)~{\rm kJ/mol}$ . On Pt(111), phenol adsorbs 351 molecularly at 90 K with a decreasing heat of adsorption in 352 the first 0.15 ML well fit by  $-\Delta H_{\rm ad} = (220-808~\theta)~{\rm kJ/mol}$ . On 353 both Ni(111) and Pt(111), phenol adsorbs with a nearly 354 constant heat of adsorption above 0.3 ML of 72–74 kJ/mol, 355 which is the value for multilayer solid phenol. Using the known 356 enthalpies of the gas-phase phenol, we find a standard enthalpy 357 of formation of adsorbed phenol  $(\Delta H_{\rm f}^0)$  of  $-272~{\rm kJ/mol}$  on 358 Ni(111) and  $-271~{\rm kJ/mol}$  on Pt(111).

These measured energies were compared to DFT from many different studies. We found that DFT calculations that neglect van der Waals corrections are more likely to underestimate this adsorption energy, while many DFT functionals that include van der Waals corrections are more accurate. However, some calculations on both surfaces, even those with vdW corrections, still grossly underestimated the adsorption energy of phenol.

# 66 AUTHOR INFORMATION

667 Corresponding Author

368 \*E-mail: charliec@uw.edu.

369 ORCID ®

370 Wei Zhao: 0000-0001-5407-6164

371 Charles T. Campbell: 0000-0002-5024-8210

372 Notes

373 The authors declare no competing financial interest.

## 74 ACKNOWLEDGMENTS

375 The authors acknowledge support for this work by the National 376 Science Foundation under CHE-1665077. We also thank Kuan 377 Chen for his assistance in the laboratory. S.J.C. is greatly 378 indebted to Prof. H.-J. Freund for being a wonderful mentor for 379 the several months he worked at the Fritz-Haber Institute 380 during his graduate studies. C.T.C. is also extremely grateful to

Prof. Freund for his support on many occasions, for decades of 381 productive and exciting scientific collaborations and discus- 382 sions, for his selfless service, which has greatly benefitted 383 everyone in the scientific community, and for being a great and 384 valued friend. C.T.C. is also very grateful to Prof. Joachim Sauer 385 for his friendship, lively scientific discussion, and many 386 contributions to the scientific community.

### REFERENCES

- (1) Singh, N.; Song, Y.; Gutiérrez, O. Y.; Camaioni, D. M.; Campbell, 389 C. T.; Lercher, J. A. Electrocatalytic Hydrogenation of Phenol over 390 Platinum and Rhodium: Unexpected Temperature Effects Resolved. 391 ACS Catal. 2016, 6 (11), 7466–7470.
- (2) Zhao, C.; He, J.; Lemonidou, A. A.; Li, X.; Lercher, J. A. Aqueous-393 Phase Hydrodeoxygenation of Bio-Derived Phenols to Cycloalkanes. *J.* 394 Catal. **2011**, 280 (1), 8–16.
- (3) Zhao, C.; Kou, Y.; Lemonidou, A. A.; Li, X.; Lercher, J. A. 396 Hydrodeoxygenation of Bio-Derived Phenols to Hydrocarbons Using 397 RANEY® Ni and Nafion/SiO 2 Catalysts. *Chem. Commun.* **2010**, 46 398 (3), 412–414.
- (4) Song, Y.; Gutiérrez, O. Y.; Herranz, J.; Lercher, J. A. Aqueous 400 Phase Electrocatalysis and Thermal Catalysis for the Hydrogenation of 401 Phenol at Mild Conditions. *Appl. Catal., B* **2016**, 182 (11), 236–246. 402 (5) Ilikti, H.; Rekik, N.; Thomalla, M. Electrocatalytic Hydrogenation 403 of Phenol in Aqueous Solutions at a Raney Nickel Electrode in the 404 Presence of Cationic Surfactants. *J. Appl. Electrochem.* **2002**, 32 (6), 405 603–609.
- (6) Myers, A. K.; Benziger, J. B. Effect of Substituent Groups on the 407 Interaction of Benzene with nickel (111). *Langmuir* **1989**, *5* (6), 1270–408
- (7) Zhuang, S. X.; Wei, X. M.; Wang, Y. S.; Zhai, R. S. A HREELS 410 Study of the Interaction of Cyclohexanone and Phenol with Pt(111) 411 Surface. *Chin. Chem. Lett.* **1996**, 7 (7), 661–662.
- (8) Lu, F.; Salaita, G. N.; Laguren-Davidson, L.; Stern, D. A.; 413 Wellner, E.; Frank, D. G.; Batina, N.; Zapien, D. C.; Walton, N.; 414 Hubbard, A. T. Characterization of Hydroquinone and Related 415 Compounds Adsorbed at Pt(111) from Aqueous Solutions: Electron 416 Energy-Loss Spectroscopy, Auger Spectroscopy, LEED, and Cyclic 417 Voltammetry. *Langmuir* 1988, 4 (3), 637–646.
- (9) Ihm, H.; White, J. M. Stepwise Dissociation of Thermally 419 Activated Phenol on Pt(111). *J. Phys. Chem. B* **2000**, 104 (26), 6202–420 6211.
- (10) Ajo, H. M.; Ihm, H.; Moilanen, D. E.; Campbell, C. T. 422 Calorimeter for Adsorption Energies of Larger Molecules on Single 423 Crystal Surfaces. *Rev. Sci. Instrum.* **2004**, *75* (11), 4471–4480.
- (11) Lew, W.; Lytken, O.; Farmer, J. A.; Crowe, M. C.; Campbell, C. 425 T. Improved Pyroelectric Detectors for Single Crystal Adsorption 426 Calorimetry from 100 to 350 K. Rev. Sci. Instrum. 2010, 81 (2), 427 024102.
- (12) Lytken, O.; Lew, W.; Harris, J. J. W.; Vestergaard, E. K.; 429 Gottfried, J. M.; Campbell, C. T. Energetics of Cyclohexene 430 Adsorption and Reaction on Pt(111) by Low-Temperature Micro-431 calorimetry. J. Am. Chem. Soc. 2008, 130 (31), 10247–10257.
- (13) Carey, S. J.; Zhao, W.; Frehner, A.; Campbell, C. T.; Jackson, B. 433 Energetics of Adsorbed Methyl and Methyl Iodide on Ni(111) by 434 Calorimetry: Comparison to Pt(111) and Implications for Catalysis. 435 ACS Catal. 2017, 7 (2), 1286–1294.
- (14) Stuckless, J. T.; Frei, N. A.; Campbell, C. T. Pyroelectric 437 Detector for Single-Crystal Adsorption Microcalorimetry: Analysis of 438 Pulse Shape and Intensity. Sens. Actuators, B 2000, 62 (1), 13–22. 439 (15) King, D. A. Molecular Beam Investigation of Adsorption 440
- (15) King, D. A. Molecular Beam Investigation of Adsorption 440 Kinetics on Bulk Metal Targets: Nitrogen on Tungsten. J. Vac. Sci. 441 Technol. **1972**, 9 (2), 905.
- (16) Carey, S. J.; Zhao, W.; Campbell, C. T. Energetics of Adsorbed 443 Benzene on Ni(111) and Pt(111) by Calorimetry. *Surf. Sci.* **2018**, 444 DOI: 10.1016/j.susc.2018.02.014.

The Journal of Physical Chemistry C

- 446 (17) Weinberg, W. H.; Merrill, R. P. A Simple Classical Model for 447 Trapping in Gas—Surface Interactions. *J. Vac. Sci. Technol.* **1971**, 8 (6), 448 718—724.
- 449 (18) Silbaugh, T. L.; Campbell, C. T. Energies of Formation 450 Reactions Measured for Adsorbates on Late Transition Metal Surfaces. 451 *J. Phys. Chem. C* **2016**, *120* (44), 25161–25172.
- 452 (19) Parsons, G. H.; Rochester, C. H.; Wood, C. E. C. Effect of 4-453 Substitution on the Thermodynamics of Hydration of Phenol and the 454 Phenoxide Anion. *J. Chem. Soc. B* **1971**, 533.
- 455 (20) Cox, J. D. The Heats of Combustion of Phenol and the Three 456 Cresols. *Pure Appl. Chem.* 1961, 2 (1-2), 125.
- 457 (21) Andon, R. J. L.; Biddiscombe, D. P.; Cox, J. D.; Handley, R.; 458 Harrop, D.; Herington, E. F. G.; Martin, J. F. 1009. Thermodynamic 459 Properties of Organic Oxygen Compounds. Part I. Preparation and 460 Physical Properties of Pure Phenol, Cresols, and Xylenols. *J. Chem. Soc.* 461 **1960**, 5246.
- 462 (22) Redhead, P. A. Thermal Desorption of Gases. *Vacuum* **1962**, 12 463 (4), 203–211.
- 464 (23) Gottfried, J. M.; Vestergaard, E. K.; Bera, P.; Campbell, C. T. 465 Heat of Adsorption of Naphthalene on Pt(111) Measured by 466 Adsorption Calorimetry. J. Phys. Chem. B 2006, 110 (35), 17539–467 17545.
- 468 (24) Zhao, W.; Carey, S. J.; Morgan, S. E.; Campbell, C. T. 469 Energetics of Adsorbed Formate and Formic Acid on Ni(111) by 470 Calorimetry. *J. Catal.* **2017**, *352*, 300–304.
- 471 (25) Delle Site, L.; Alavi, a.; Abrams, C. Adsorption Energies and 472 Geometries of Phenol on the (111) Surface of Nickel: An Ab Initio 473 Study. *Phys. Rev. B: Condens. Matter Mater. Phys.* **2003**, 67 (19), 1–3. 474 (26) Yoon, Y.; Rousseau, R.; Weber, R. S.; Mei, D.; Lercher, J. A. 475 First-Principles Study of Phenol Hydrogenation on Pt and Ni Catalysts 476 in Aqueous Phase. *J. Am. Chem. Soc.* **2014**, 136 (29), 10287–10298. 477 (27) Honkela, M. L.; Björk, J.; Persson, M. Computational Study of
- 478 the Adsorption and Dissociation of Phenol on Pt and Rh Surfaces.
  479 Phys. Chem. Chem. Phys. 2012, 14 (16), 5849.
  480 (28) Li, G.; Han, J.; Wang, H.; Zhu, X.; Ge, Q. Role of Dissociation
- 481 of Phenol in Its Selective Hydrogenation on Pt(111) and Pd(111). 482 ACS Catal. **2015**, 5 (3), 2009—2016. 483 (29) Peköz, R.; Donadio, D. Effect of van Der Waals Interactions on
- 484 the Chemisorption and Physisorption of Phenol and Phenoxy on 485 Metal Surfaces. *J. Chem. Phys.* **2016**, *14*5 (10), 104701. 486 (30) Réocreux. R.: Huynh. M.: Michel, C.: Sautet, P. Controlling the
- 486 (30) Réocreux, R.; Huynh, M.; Michel, C.; Sautet, P. Controlling the 487 Adsorption of Aromatic Compounds on Pt(111) with Oxygenate 488 Substituents: From DFT to Simple Molecular Descriptors. *J. Phys.* 489 Chem. Lett. **2016**, 7 (11), 2074–2079.
- 490 (31) Yaws, C. L. Yaw's Handbook of Thermodynamic and Physical 491 Properties of Chemical Compounds; Knovel: 2003.